CHAPTER 1

INTRODUCTION

INTRODUCTION

1.1 Background information and research significance

Nanotechnology is the branch of science that deals with dimensions less than 100 nm. It can be defined as ñNanoscience and technology is the study of phenomena and manipulation of materials at atomic, molecular and macromolecular scales, where properties differ significantly from those at the larger scaleò [1]. This new technology alters the way we perceive the scientific world as it effaces the boundaries between physics, chemistry and biology. Nevertheless, the elimination of these boundaries will pose many challenges and new directions for the organization of education and research [2]. The integration of nanotechnology with medicine has resulted in active developments of the new emerging research area, nanobiotechnology, which offers exciting opportunities for discovering new materials, processes, and phenomena. At this particular dimension, the nanoparticles exhibit peculiar properties which are very different from their bulk equivalents. This is because nanoscale materials possess a larger surface to volume ratio than the bulk materials and when the surface area per mass of the material increases, a greater amount of the material can come into contact with surrounding materials, hence making them highly reactive. As a result, nanoscale materials have found their use in various areas such as biomedical imaging, therapeutics, magnetic recording, catalysis, waste water treatment, energy etc. [3-8].

Nanobiotechnology is a young and rapidly growing field formed by the unification of two very dissimilar worlds of biotechnology and nanotechnology [9, 10]. This new branch of science concerns with the ability to create and manipulate biological and biochemical materials, devices, and systems at atomic and molecular levels. This hybrid discipline also involves the refinement and application of instruments, originally designed to generate and manipulate nanostructured materials, to basic and applied studies of fundamental biological processes. This technology holds the considerable promise of advances in various biomedical applications, not only in drug delivery and gene therapy but also in molecular imaging, biomarkers and biosensors [11-14]. Some potential biomedical applications of the nanosystems are expressed in **figure 1.1.**

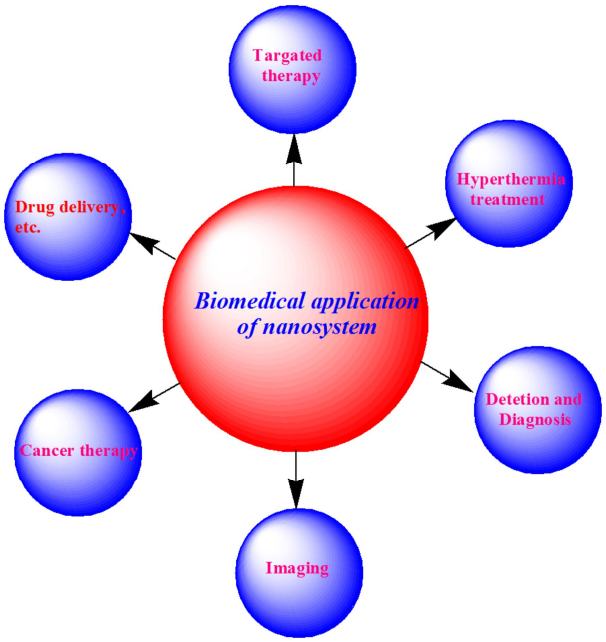

Figure 1.1 Biomedical applications of nanosystem

1.1.1 Magnetic nanosystems

Magnetic nanoparticles are of immense technological importance because of their applications in a wide range of areas like in magnetic fluids, catalysis, biomedicine, magnetic resonance imaging, data storage, and environmental remediation [15-18]. Magnetic nanoparticles possess remarkable properties such as superparamagnetism, high field irreversibility, high saturation field, extra anisotropy contributions or shifted loops after field cooling. Superparamagnetism (SP) describes the state of a single-domain-sized grain when thermal energy is sufficient to overcome barriers to a reversal of magnetization. When the energy barriers are large with respect to thermal energy, the 9 magnetization is ñblockedò and the probability of spontaneous reversal becomes negligible. When the barriers are relatively low, thermal excitations can result in reversal of the magnetization over very short time scales, and the grain is in a superparamagnetic state. The behavior of superparamagnetic nanoparticles can be described by the Langevin equation ($M/M_s = \coth \check{U} - 1/\check{U}$, where, $\check{U} = \varepsilon_o mH/k_B T$ the ratio of magnetic to thermal energy), where H is the magnetic ýeld, and m is the magnetic moment of a single particle, k_B is the Boltzmann constant). Retentivity is the magnetization left behind in a ferromagnetic material after an external magnetic field is

removed whereas coercivity is the intensity of the applied magnetic field required to reduce the magnetization of that material to zero from saturation. In the superparamagnetic condition, the net magnetization is zero, in the absence of an external field whereas the retentivity and coercivity of a system is ideally zero or close to zero at particular temperature with the external field.

The magnetic behavior of individual nanoparticles is dominated by two key effects: finite size effect and surface effect [19]. Due to their interesting magnetic properties, nanoscale magnetic materials provide many exciting opportunities in biomedical applications [20]. First, due to their controllable sizes ranging from a few up to tens of nanometers, it is possible to tailor their properties in view of the proposed study. Secondly, the nanoparticles can be manipulated by an external magnetic force which is advantageous for many applications. Third, magnetic nanoparticles have great potential as MRI contrast enhancement agents because the signal of the magnetic moment of a proton around magnetic nanoparticles can be captured by resonant absorption.

Different methods have been exploited for the development of magnetic nanoparticles of various different compositions. However, due to the inherent magnetic properties of the magnetic nanoparticles they tend to agglomerate and hence the successful application of these magnetic nanoparticles relies highly on the stability of these nanoparticles on various conditions. The popular methods used for the synthesis of high-quality magnetic nanoparticles include co-precipitation, thermal decomposition and/or reduction, micelle synthesis, hydrothermal synthesis, and laser pyrolysis techniques [21-24].

1.1.2 Quantum dots

Quantum dots (QDs), often regarded as ‘artificial atoms’, are semiconductor crystals composed of group II to VI or III to V elements in which electronic excitations are confined [25]. In semiconductor QDs, the excitons are confined in all three spatial dimensions. These QDs are smaller than their exciton Bohr radius (about 1 to 5 nm). Due to their very small confined dimension, it is popularly known as ‘zero-dimension’. Owing to their small size, QDs displays intriguing electronic properties very different

from their bulk counterparts. With the tuning of their size, QDs can adopt new and exciting properties. The most amazing size-dependent property exhibited by the QDs is the modulation of the absorbance and emission with the alteration in size, fundamentally known as quantum confinement and hence the name ǿquantum dotô[2, 26]. Due to their unique size and composition tunable electronic property, these fine semiconductor quantum dots are employed in a variety of applications and new technologies. Owing to their ability to emit a rainbow of colours coupled with high efficiencies, longer lifetimes and high extinction coefficient, quantum dots are particularly significant for optical applications such as LEDs and solid state lighting, displays and photovoltaic [27, 28]. The unique electronic architecture of the zero- dimensional quantum dots paves way to unique electronic properties which can be used in transistors, solar cells, ultrafast all-optical switches and logic gates, and quantum computing, among many others [29, 30]. Being zero-dimensional, the quantum dots have the advantage to reach any parts of the body which make them suitable for various biomedical applications like medical imaging, biosensors, etc.

Several methods have been used for the synthesis of QDs which are broadly classified into top-down and bottom-up approaches. The top-down approaches generally include molecular beam epitaxy (MBE), ion implantation, e-beam lithography, reactive ion etching and X-ray lithography [31, 32]. While in case of bottom-up approaches different self-assembly techniques are employed which are broadly classified into wet-chemical and vapour-phase methods. Microemulsion, sol-gel, competitive reaction chemistry, hot-solution decomposition, and electrochemistry generally fall under the category of wet-chemical methods. Self-assembly of nanostructures developed by molecular beam epitaxy (MBE), sputtering, liquid metal ion sources, or aggregation of gaseous monomers are classified as vapour-phase methods [33-35].

1.1.3 Molecular Imaging

Magnetic contrast imaging and contrast agents

The conventional imaging platforms/techniques used in both clinical and research applications to map the tissues and organs in the body, includes computed X-ray tomography (CT), optical imaging, magnetic resonance imaging (MRI), positron emission tomography (PET), single-photon-emission computed tomography (SPECT),

and ultrasound [36-39]. These techniques exhibit the advantages of real-time imaging of the cellular functions of living organisms and related molecular interactions and most importantly, these techniques are noninvasive. Of all these techniques, magnetic resonance imaging (MRI) has evolved as a promising non-invasive technique because of its ability to acquire 3D tomographical information in whole tissue samples, including human soft tissues and whole animals, at high spatial and temporal resolution. In addition to these, as MRI works without the use of carcinogenic ionizing radiation (X-ray/CT) or radiotracers (PET and SPECT), it reigns as the most preferred imaging technique for the heart, brain, and nervous system. In order to differentiate between normal and diseased cells, MRI contrast agents are used in order to enhance the contrast.

An MR image typically made up of voxels demonstrating the nuclear magnetic resonance (NMR) signal intensity of the hydrogen atoms in water and fat of living organisms. The atom with a net nuclear spin can be used for MRI like ^{3}He, ^{13}C, ^{19}F, ^{17}O, ^{23}Na, ^{31}P, and ^{129}Xe. The hydrogen atom (^{1}H) is most widely employed because it is abundant in biological tissues. In a magnetic ýeld, the hydrogen nuclear spins align with (parallel) or against (antiparallel) the external magnetic ýeld (B_0) (**figure 1.2**). The magnetic dipole (μ) is generated by spinning of the proton about its axis. An external field (B_0) produces a torque (Ű resulting in its precession at angular Larmor frequency ($ɤ_0$). Larmor frequency is expressed as $ɤ_0 = ɔB_0$. The difference in the populations of parallel and antiparallel protons is determined by the energy difference (ɸE) between two states. The energy difference is calculated by following equation-

$$ɸE = \frac{ɔhB_0}{2´}$$

Where, ɔ = proton gyromagnetic ratio, h = Plankôs constant.

The excess proton population is so small that only 0.001 % of hydrogen is detected, that is why MRI has relatively low sensitivity. However, the signal intensity can be enhanced by employing a high-ýeld MRI scanner because the energy difference increases with the external magnetic ýeld.

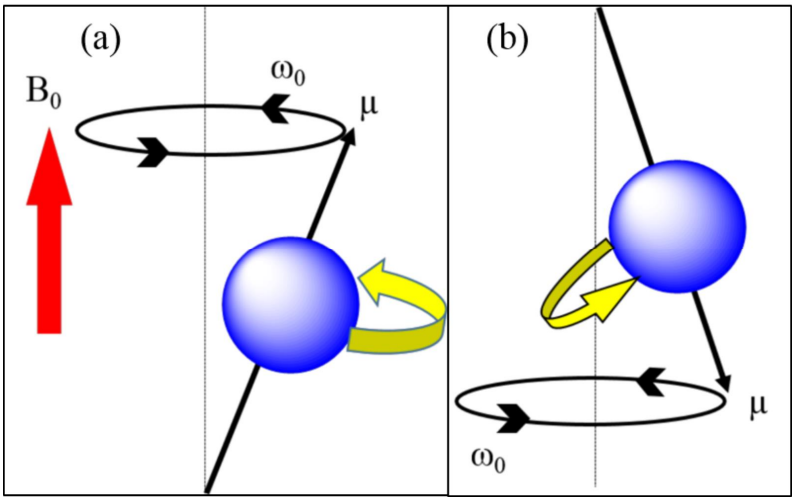

Figure 1.2 Schematic diagram represents the hydrogen nuclear spins in external magnetic ýeld (a) parallel (b) antiparallel

The basic principle (**figure 1.3**) of MRI is based upon the response of proton spin in the presence of an external magnetic field when triggered with a radio frequency (RF) pulse [40].

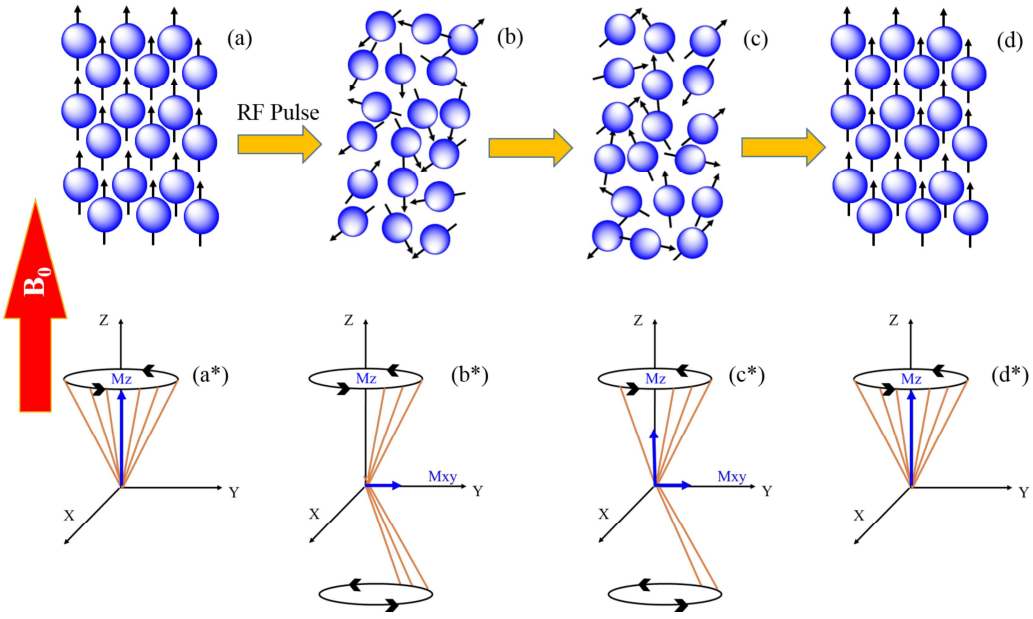

Figure 1.3 Schematic diagram showing the principle of proton relaxation

When an external magnetic field is applied, the protons align themselves in one direction (**figure 1.3 a & a***). On application of the RF pulse, the aligned protons are

absorbed the electromagnetic energy, and the antiparallel spin population increases. Therefore, longitudinal magnetization (parallel to the external magnetic ýeld) decreases and transverse magnetization (perpendicular to the external magnetic ýeld) is generated (**figure 1.3 b & b***). When the RF pulse is off, the nuclear spins return to their initial state, which is termed as relaxation (**figure 1.3 c, c* and d, d*)**. Relaxation is the process in which spins release the energy received from a radiofrequency pulse. The proton spin density and the two independent relaxation processes, longitudinal (T_1) and transverse (T_2) relaxation times, plays the major role in generating the contrast in the MR images. T_1 relaxation is the recovery of longitudinal orientation. Time T_1 refer to the interval where 63% of the longitudinal magnetization is recovered whereas T_2 relaxation is a process of dephasing where loss of transverse magnetization occurs. Time T_2 refers to the interval where only 37 % of original transverse magnetization is attained (**refer figure 1.4**). Depending upon the relaxation processes involved, there are two varieties of contrast agents involved in enhancing the contrast in the MR images: (i) T_1-weighted contrast agents and (ii) T_2- weighted contrast agents. On the basis of contrast, there are two types of images (a) T_1 weighted image and (b) T_2 weighted image. T_1 is primarily influenced by repetition time (TR) whereas T_2 by echo-time (TE). The spin echo sequences are presented in the inset of **figure 1.4 (b)**. The repetition time (TR) is the time interval between applications of 90° radiofrequency pulse whereas echo time (TE) is the time between the initial 90° radiofrequency pulse and the measurement. T_1-weighted image tends to have short TE and TR times. The MR signal intensity (I) of the spin echo sequence associated with TE and TR can be expressed by following equation-

$$I = M_o\left[1-\exp\left(-\frac{T_R}{T_1}\right)\right]\exp\left(-\frac{T_E}{T_2}\right)$$

(M_0 = Total magnetization)

T_1-weighted image is used to differentiate anatomical structures mainly on the basis of T_1 values; i.e. the scanning parameters are set (short TR / short TE) to minimize T_2 relaxation effects. Tissues with high-fat content appear bright and compartments filled with water appears dark. This is the principle for demonstrating anatomy.

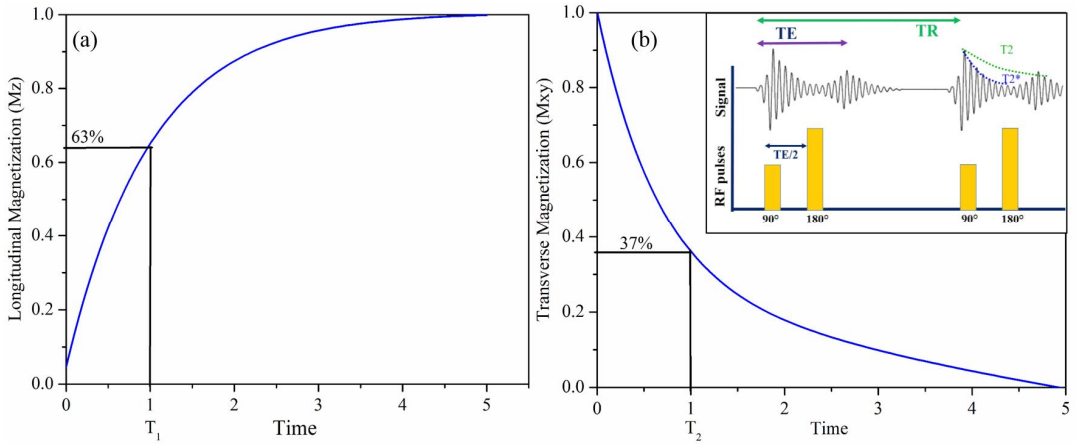

Figure 1.4 Schematic showing T_1 and T_2 relaxation dynamics and inset reveal spin echo sequences

T_2-weighted imaging is used to differentiate anatomical structures mainly on the basis of T_2 values; i.e. the scanning parameters are set (long TR/ long TE) to minimize T_1 relaxation effects. Compartments filled with the water appear bright and tissues with high-fat content appear dark. This is the principle for demonstrating pathology since most (not all) lesions are associated with an increase in water content. When TE is short (typically TE < 30 ms) and TR (typically TR > 2000 ms) is long, neither T_1 nor T_2 is weighted. In this case, the signal intensity is proportional to a number of protons, and proton density-weighted images are acquired.

MRI contrast agent is used to improve the visibility of substance by changing the relaxation time around the agent. MRI contrast agents usually shorten both T_1 and T_2. T_1 contrast agents increase R_1 and R_2 by roughly the same amount, whereas T_2 contrast agents increase R_2 much more than R_1. T_1 contrast agents are positive contrast agents since they shorten T_1, which increases the signal intensity in T_1-weighted images. On the other hand, T_2 contrast agents are negative contrast agents because their T_2 contrast effect reduces the signal intensity in T_2-weighted images. The T_1-weighted contrast agents are the gadolinium (Gd^{3+}) and manganese (Mn^{2+}) based chelates, which are generally paramagnetic in nature. On the other hand, the T_2-weighted contrast agents are superparamagnetic materials which shorten T_2 (increase r_2), leading to dark contrast T_2-weighted images. The efficiency of a contrast agent to reduce the relaxation times T_1 or

T_2 of water protons are referred to as relaxivity and are expressed in terms of the following equation:

$$R_i = \frac{1}{T_i} = \left(\frac{1}{Ti}\right)_0 + r_i C$$

Where R_i is the relaxation rate of the aqueous solution, T_{i0} is the relaxation time in the absence of the contrast agent, C is the concentration of the contrast agent, and r_i is its relaxivity.

With the increasing popularity of MRI as a non-invasive and highly sensitive imaging technique, there has been a significant increase in the demand of novel nanomaterials as MRI contrast agents. It is because nanomaterial-based MRI contrast agents offer a number of advantages over the conventional contrast agents, such as (1) stability and tunable biodistribution can be obtained by surface engineering; (2) biocompatibility and imaging properties can be tuned by varying the chemical composition, shapes, and sizes; (3) identification of the target area by specific conjugation with biological molecules interactions, such as antibodies, nucleic acids, and peptides; and (4) multimodal imaging can also be achieved.

1.1.4 Fluorescence imaging and fluorescent imaging probes

Optical imaging and spectroscopy are very popular and demanding in the field of medicine and biomedical technology because of the compactness, low cost, and ability of the technology to provide functional and molecular information [41, 42]. When light interacts with biological tissues, a number of photophysical events occur within the tissues such as absorption, scattering, and emission of light. A great deal of biochemical and morphological information about the targeted tissue can be derived from each of these events. Using the contrast mechanisms of these optical methods several optical imaging platforms have been established that include spectroscopic, planar, diffuse, and hybrid biomedical optics methods.

The basic principle of fluorescence imaging lies in the absorption and emission of light by endogenous or exogenous chromophore resulting into a contrast between the

diseased and normal surrounding tissue [43]. Because of its capacity for a wide range of spatial imaging from cells to organ systems, it has evolved out as an important technology for medical imaging. In fluorescence imaging instruments, the imaging probes generally have fluorescence or bioluminescence properties to enhance the image contrast. The cells and tissues have innate autofluorescence which can be considered as the simplest form of contrast agents. However, this innate fluorescence is not sufficient enough for detection of tumor lesions in an early stage. Therefore, development of novel, highly sensitive, and specific imaging probes for fluorescence imaging is an important requisite for the development of optical imaging techniques.

1.1.5 Multimodal imaging and different types of multimodal systems

Own pros and cons have associated with each imaging technique, in the biomedical imaging field. Based on such fact, with the development of multimodal imaging technology has attracted great attention in the scientific community in recent time. The present research trend shows immense interest in the development of multimodality imaging, as no single imaging modality has all of the ideal characteristics of being quantitative and longitudinal and at the same time providing both high resolution and sensitivity. Because of their highly complementary capabilities for anatomical resolution and detection sensitivity, the combination of non-ionizing magnetic resonance imaging (MRI) and optical techniques have been considered as the most suitable candidate. The hybrid modality has shown potential for superior diagnostic accuracy compared to the already prevalent fluorescence techniques and is stirring up a huge interest in the domain of multifunctional materials that can be detected by both modalities. Multifunctional nanostructures consisting of two or more functional components have opened up new vistas in the field of multimodal imaging. Through bottom-up approach it is possible to design new routes for the synthesis of such novel types of hybrid nanomaterials, in which the assemblage of the unique functions (mainly magnetic, optic, and/or electronic properties) and the synergy between the intrinsic properties of the components are engineered within a single system. Consequently, the multifunctional hybrid nanosystems for multimodal imaging are broadly classified into three different categories: fluorescent-magnetic systems, fluorescent-plasmonic systems, and magnetic-plasmonic systems. Surface plasmons are collective oscillations of free

electrons in metallic surfaces and particles. Plasmonic NPs exhibiting localized surface plasmon resonances can show strong optical resonances for visible and near-infrared wavelengths. This is due to the collective oscillations of free conduction electrons when illuminated with light at the plasmon wavelength (λ_{max}). The metal-enhanced fluorescence (fluorescent-plasmonic) phenomenon is a result of the interaction between excited states of the fluorophores and the induced surface plasmons of metal nanoparticles. Plasmon nanostructures are known to efficiently enhance the fluorescence of the surrounding fluorophores. The mechanism of plasmon enhancement can be mainly attributed to the increased excitation rate due to a local field enhancement effect and the increased emission rate by surface plasmon coupled emission, which can enhance both the quantum yield and fluorescence intensity. Magnetic-plasmonic nanoparticles combining magnetic and plasmonic components are promising structures are commonly called ñtheranosticò structures in biomedical contexts due to their therapeutic and diagnostic potentials [44-47]. These hybrid nanosystems can be used in multidisciplinary biomedical applications, such as fluorescence imaging combined with MRI and visible multiple cell tracking and separation [48, 49].

1.2 Aspects of literature review and objective of the thesis

Based on the above literature review, the importance of multimodal magneto-fluorescent hybrid nanosystem has been established in the field of biomedical applications. It is seen that the development of magneto-fluorescent nanomaterials that simultaneously exhibit superior magnetic property, enhanced fluorescence capability, and a versatile surface functionality is quite challenging.

During the course of my doctoral research project, the most intriguing task was to incorporate both magnetic and fluorescent components in a single system without compromising on both the aspects. Keeping the uphill task in mind, I have attempted to develop a set of magnetic NPs, quantum dots (QDs), and magneto-fluorescent hybrid nanosystems using the bottom-up approach. The physicochemical and biomedical properties of magnetic and QDs were studied. By varying of the fluorescent components, different combinations of magneto-fluorescent hybrids were developed (**refer figure 1.5**). Moreover, developing magneto-fluorescent hybrids nanosystem

through a simple, one-pot synthesis procedure is explored in the thesis work. Finally, the multimodalities of these developed magneto-fluorescent systems are examined in Magnetic Resonance (MR) and Fluorescence Imaging (FI) applications. The materials developed and methods applied in the thesis are shown as a schematic diagram in **figure 1.5**.

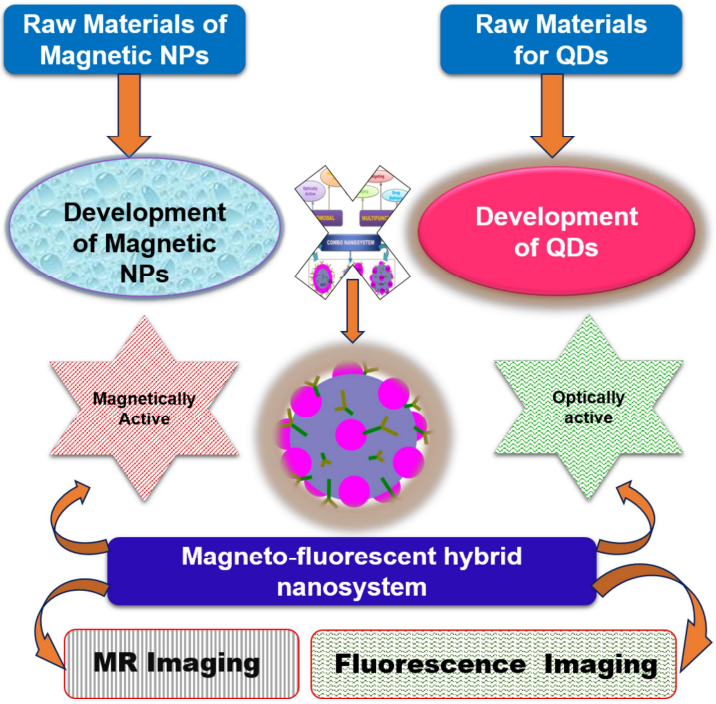

Figure 1.5 Schematic diagram representing the development of magneto-fluorescent hybrid nanosystem and applications of these nanosystems in imaging

The following objectives have been outlined based on past, present and future prospects:

1. Development and characterization of an array of magnetic nanosystems for hybrid conjugation.
2. Synthesis and characterization of an array of quantum dots for hybrid conjugation.
3. Identification and stable hybridization of precursor nanosystems to obtain multimodal nanosystems.
4. Microstructural, surface, physical property and bioassay of selected hybrid nanosystems.
5. Evaluation of the efficacy of the multimodal properties amongst the selected hybrid nanosystems.

Materials developed are:

- Magnetic nanoparticles: Magnetite (Fe_3O_4) and FePt nanoparticles.
- Fluorescent nanoparticles: GSH capped CdTe, CdSe and CdS quantum dots.
- Magneto-fluorescent hybrid: GSH capped FePt@CdTe, FePt@CdSe, and FePt@CdS.

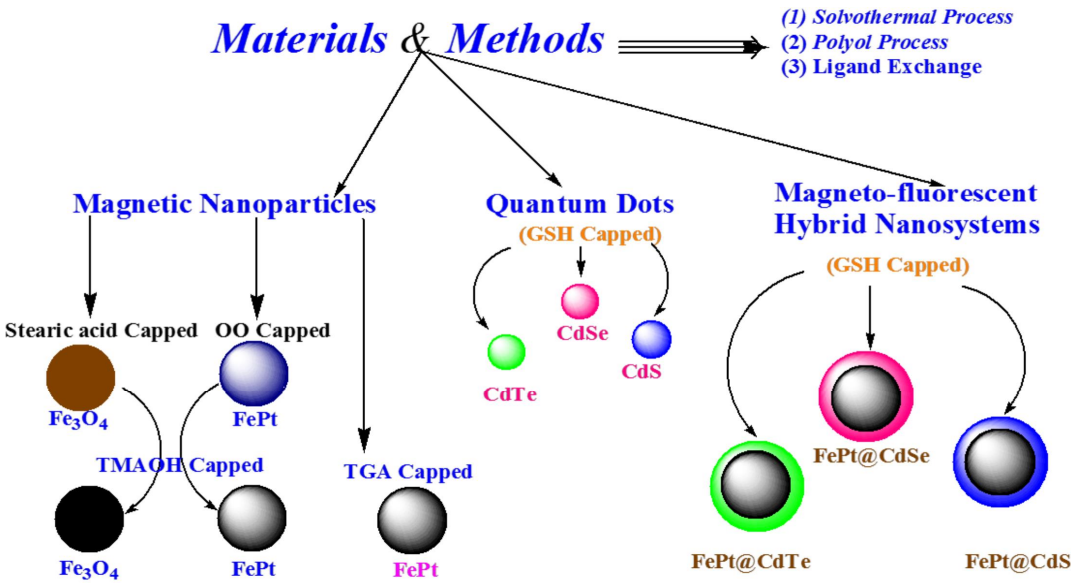

Figure 1.6 Schematic representation depicts synthesis process and the nanosystem synthesized in the present thesis

(OO-Oleic acid and Oleyl amine; TMAOH-tetramethylammonium hydroxide; TGA-thioglycolic acid; GSH-glutathione). Ligand exchange process is used for making hydrophilic surface by TMAOH capping.

References:

[1] Dowling, A. *et al.* Nanoscience and nanotechnologies؛ opportunities and uncertainties. *London R. Soc. R. Acad. Eng. Rep.* **46** (July), 618--618, 2004

[2] Taylor-Pashow, K. M. L. *et al.* Hybrid nanomaterials for biomedical applications. *Chem. Commun. (Camb).* **46** (32), 5832--5849, 2010.

[3] Liu, F. *et al.* Superparamagnetic nanosystems based on iron oxide nanoparticles for biomedical imaging. *Nanomedicine (Lond).* **6** (3), 519--528, 2011.

[4] Kim, T. & Hyeon, T. Applications of inorganic nanoparticles as therapeutic agents. *Nanotechnology* **25** (1), 012001--012014, 2014.

[5] Wang, J. P. FePt magnetic nanoparticles and their assembly for future magnetic media. *Proc. IEEE* **96** (11), 1847--1863, 2008.

[6] Jain, K. K. Nanomedicine: Application of nanobiotechnology in medical practice. *Medical Principles and Practice* **17** (2), 89--101, 2008.

[7] Tang, S. C. N. & Lo, I. M. C. Magnetic nanoparticles: Essential factors for sustainable environmental applications. *Water Research* **47** (8), 2613--2632, 2013.

[8] Lee, S. H. *et al.* Metal oxide nanoparticles for advanced energy applications. *Thin Solid Films* **517** (12), 3591--3595, 2009.

[9] Li, X. & Que, L. Fluorescence Enhancement Enabled by Nanomaterials and Nanostructured Substrates: A Brief Review. *Rev. Nanosci. Nanotechnol*. **3** (3), 161--176, 2014.

[10] Whitesides, G. M. The órightô size in nanobiotechnology. *Nat. Biotechnol.* **21** (10), 1161--1165, 2003.

[11] McBain, S. C. *et al*. Magnetic nanoparticles for gene and drug delivery. *International Journal of Nanomedicine* **3** (2)**,** 169--180, 2008.

[12] Liu, C. & Zhang, N. Nanoparticles in gene therapy: Principles, prospects, and challenges. *Progress in Molecular Biology and Translational Science* **104**, 509--562, 2011.

[13] Minchin, R. F. & Martin, D. J. Nanoparticles for molecular imaging--an overview. *Endocrinology* **151** (2), 474--481, 2010.

[14] Haun, J. B. *et al.* Molecular detection of biomarkers and cells using magnetic nanoparticles and diagnostic magnetic resonance. *Methods Mol Biol* **726**, 33--49, 2011.

[15] Zhang, G. *et al.* Surface engineering of core/shell iron/iron oxide nanoparticles from microemulsions for hyperthermia. *Mater. Sci. Eng. C* **30** (1), 92--97, 2010.

[16] Antoniak, C. *et al.* A guideline for atomistic design and understanding of ultrahard nanomagnets. *Nat. Comm.* **2**, 528--534, 2011.

[17] Thapa, D. *et al.* Properties of magnetite nanoparticles synthesized through a novel chemical route. *Mater. Let.* **58** (21), 2692--2694, 2004.

[18] Frey, N. A. *et al.* Magnetic nanoparticles: synthesis, functionalization, and applications in bioimaging and magnetic energy storage. *Chem. Soc. Rev.* **38** (9), 2532--2542, 2009.

[19] Issa, B. *et al.* Magnetic nanoparticles: Surface effects and properties related to biomedicine applications. *Int. J. of Mol. Sci.* **14** (11), 21266--21305, 2013.

[20] Pankhurst, Q. A. *et al.* Applications of magnetic nanoparticles in biomedicine. *J. of Phy. D: Appl. Physi.* **36** (13), R167--R181, 2003.

[21] Jha, D. K. *et al.* Simple synthesis of superparamagnetic magnetite nanoparticles as highly efficient contrast agent. *Mater. Lett.* **95**, 186--189, 2013.

[22] Qin, C. *et al.* Facile synthesis of magnetic iron oxide nanoparticles using 1-methyl-2-pyrrolidone as a functional solvent. *Colloids Surfaces A Physicochem. Eng. Asp.* **336** (1), 130--134, 2009.

[23] Mascolo, M. C. *et al.* Room Temperature Co-Precipitation Synthesis of Magnetite Nanoparticles in a Large ph Window with Different Bases. *Materials (Basel).* **6** (12), 5549--5567, 2013.

[24] Veintemillas-Verdaguer, S. *et al.* Colloidal dispersions of maghemite nanoparticles produced by laser pyrolysis with application as NMR contrast agents. *J. of Phy. D: Appl. Phy.* **37** (15), 2054--2059, 2004.

[25] Hawrylak, P. Excitonic artificial atoms: Engineering optical properties of quantum dots. *Physical Rev. B* **60** (8), 5597--5608, 1999.

[26] Baskoutas, S. & Terzis, A. F. Size-dependent band gap of colloidal quantum dots. *J. Appl. Phys.* **99** (1), 13708--13711, 2006.

[27] Sun, Q. *et al.* Bright, multicoloured light-emitting diodes based on quantum dots. *Nat. Photonics* **1** (12), 717--722, 2007.

[28] Chen, H. S. *et al.* White-light emission from organics-capped ZnSe quantum dots and application in white-light-emitting diodes. *Appl. Phys. Lett.* **86** (13), 1--3, 2005.

[29] Pacifici, D. *et al.* All-optical modulation by plasmonic excitation of CdSe quantum dots. *Nat. Photonics* **1** (7), 402--406, 2007.

[30] Nakamura, H. *et al.* Ultra-fast photonic crystal/quantum dot all-optical switch for future photonic networks. *Optical Express **12*** (26), 6606--6614, 2004.

[31] Biswas, A. *et al.* Advances in top-down and bottom-up surface nanofabrication: Techniques, applications & future prospects. *Adv. in Colloid and Interface Sci.* **170** (1), 2--27, 2012.

[32] Hoffmann, S. *et al.* Axial p-n junctions realized in silicon nanowires by ion implantation. *Nano Lett.* **9** (4), 1341--1344, 2009.

[33] Suraprapapich, S. *et al.* Self-assembled quantum-dot molecules by molecular-beam epitaxy. *J. of Vac. Sci. & Tech. B: Microelectronics and Nanometer Structures* **23** (3), 1217, 2005.

[34] Liang, Y. H. *et al.* Designing various self-assembled ZnOx quantum dots/islands on silicon with distinctive characteristics by magnetron sputter. *Cryst. Growth Des.* **9** (5), 2021--2025, 2009.

[35] Graham, J. F. *et al.* Coupled effects of ion beam chemistry and morphology on directed self-assembly of epitaxial semiconductor nanostructures. *Nanotechnology* **22** (7), 075301, 2011.

[36] Flannery, B. P. *et al.* Three-Dimensional X-ray Microtomography. *Science* **237** (4821), 1439--1444, 1987.

[37] Licha, K. & Olbrich, C. Optical imaging in drug discovery and diagnostic applications. *Advanced Drug Delivery Reviews* **57** (8), 1087--1108, 2005.

[38] Gambhir, S. S. Molecular imaging of cancer with positron emission tomography. *Nat. Rev. Cancer* **2** (9), 683--693, 2002.

[39] Brooks, D. J. Positron emission tomography and single-photon emission computed tomography in central nervous system drug development. *NeuroRx* **2** (2), 226--236, 2005.

[40] Lee N. and Hyeon T. Designed synthesis of uniformly sized iron oxide nanoparticles for efficient magnetic resonance imaging contrast agents *Chemical Society Reviews* **41**, (2), 2575--2589, 2012.

[41] Gobin, A. M. *et al.* Near-infrared resonant nanoshells for combined optical imaging and photothermal cancer therapy. *Nano Lett.* **7** (7), 1929--1934, 2007.

[42] Sau, T. K. *et al.* Properties and applications of colloidal nonspherical noble metal nanoparticles. *Adv. Mat.* **22** (16), 1805--1825, 2010.

[43] Solomon, M. *et al.* Optical imaging in cancer research: basic principles, tumor detection, and therapeutic monitoring. *Med. Princ. Pract.* **20** (5), 397--415, 2011.

[44] Brullot, W., Valev, V. K. & Verbiest, T. Magnetic-plasmonic nanoparticles for the life sciences: Calculated optical properties of hybrid structures. Nanomedicine Nanotechnology, Biol. Med. **8**, 559--568, 2012.

[45] Feng A. L. *et al.* Distance-Dependent Plasmon-Enhanced Fluorescence of Upconversion Nanoparticles using Polyelectrolyte Multilayers as Tunable Spacers. Scientific Reports **5** (7779), 1--10, 2015.

[46] Levin, C. S. *et al.* Magnetic-plasmonic core-shell nanoparticles. *ACS Nano* **3,** 1379--1388, 2009.

[47] Lim, J. & Majetich, S. A. Composite magnetic-plasmonic nanoparticles for biomedicine: Manipulation and imaging. *Nano Today* **8,** 98--113, 2013.

[48] Penet, M. F. *et al.* Applications of molecular MRI and optical imaging in cancer. *Future Med. Chem.* **2** (6), 975--988, 2010.

[49] Li, X., Zhao, D. & Zhang, F. Multifunctional upconversion-magnetic hybrid nanostructured materials: Synthesis and bioapplications. *Theranostics* **3** (5), 292--305, 2013.